

MALAYSIAN JOURNAL OF ANALYTICAL SCIENCES



Journal homepage: https://mjas.analis.com.my/

Research Article

Characterisation of Cr³⁺-doped ZnAl₂O₄ synthesised by the sol-gel method using different chelating agents

Syamsyir Akmal Senawi¹, Faizatul Farah Hatta², Muhammad Firdaus Othman¹, Hendrie Johann Muhamad Ridzwan¹, Azhan Hashim³, and Wan Aizuddin W Razali^{1*}

¹Faculty of Applied Sciences, Universiti Teknologi MARA Pahang, Jengka Campus, 26400 Bandar Tun Abdul Razak Jengka, Pahang

²Centre of Foundation Studies, Universiti Teknologi MARA, Cawangan Selangor, Kampus Dengkil 43800 Dengkil, Selangor

³Faculty Of Plantation & Agrotechnology Universiti Teknologi MARA Cawangan Melaka, Jasin Campus, 77300 Merlimau Melaka

*Corresponding author: wanaizuddin@pahang.uitm.edu.my

Received: 6 August 2024; Revised: 27 November 2024; Accepted: 1 December 2024; Published: 5 February 2025

Abstract

Chromium-doped zinc aluminate (Cr³+-doped ZnAl₂O₄) is an excellent material for optical technology applications, especially in lighting, bioimaging, and display devices. In this study, Cr³+-doped ZnAl₂O₄ samples were prepared using the sol-gel method by applying citric acid and oxalic acid as chelating agents. The samples prepared using citric acid and oxalic acid are designated as SC and SO, respectively. X-ray diffraction patterns revealed that the diffraction peaks of both samples matched with the cubic ZnAl₂O₄ spinel phase. The diffraction peaks are sharp and well-defined, indicating a high degree of structural order at long range. The crystallinity indices for the SC and SO samples are 83.40 and 86.88, respectively. This indicates the sample produced using oxalic acid has better crystallinity. Different chelating agents also resulted in different profiles of surface morphology. The SO sample consists of less agglomerated small particles and uniform surface morphology, whereas the SC sample consists of agglomerated particles with clear grain boundaries. Based on the results, the SO sample exhibits better properties. Both samples produced broad emission peaks in the blue and red regions. The CIE 1931 diagram indicates coordinates of (0.2522, 0.21113) and (0.29003, 0.27166) for the SC and SO samples, respectively. Notably, the CIE coordinates for the SO sample are close to the white region. The lifetimes for the SC and SO samples are estimated to be 0.51 ms and 0.65 ms, respectively. This material can potentially be applied as a phosphor for white lightemitting diodes, as well as for biomarker. It is expected that the properties of the sample can be further improved by varying the chromium concentration and the Zn-to-Al ratio.

Keywords: Chromium-doped zinc aluminate, phosphor, sol-gel, chelating agent

Introduction

In modern society, various electrical appliances are widely used, providing many benefits to our daily lives. Thus, it is important to develop energy-saving electrical appliances capable of greatly reducing electricity consumption. Over the past decade, there has been extensive research involving phosphor materials for white light generation known as phosphor-converted white light-emitting diodes (WLEDs). These devices are more efficient compared to traditional light bulbs. Phosphor is produced by doping certain materials with transition metals or rare-earth elements. Currently, various transition metals have been doped into various hosts,

each with their unique optical properties that are applicable in current technology.

Zinc aluminate (ZnAl₂O₄) is one of the spinel oxides with various applications, such as in optoelectronic, electronics industries, and catalytic reactions [1]. This material is characterized by its non-toxicity, low surface acidity, low-temperature sinter ability, and broad bandgap [2]. It has an energy band gap of 3.8 eV, in which Zn and Al cations are positioned at the tetrahedral and octahedral sites of the cubic structure, respectively. It is known to be a suitable host lattice for various dopants or activator atoms [3, 4]. Furthermore, ZnAl₂O₄ is also usually used as a host

material for optical activators like transition metal ions or rare-earth ions, such as Cd^{2+} [5], Cr^{3+} [6], Mn^{2+} [7], Ce^{3+} [8], Sm^{3+} [9], and Eu^{3+} [10].

ZnAl₂O₄ has been synthesized using different methods, such as the sol-gel method [11], coprecipitation-hydrothermal method [12], solidstate reaction [13], and chemical precipitation [14]. In this work, the sol-gel method was used to synthesize Cr³⁺-doped ZnAl₂O₄. Cr³⁺ was chosen as the dopant because it is widely used as a dopant for phosphor materials and gives good quantum efficiency [15]. The properties of the phosphor material are influenced by various parameters during the synthesis process. Therefore, further investigation into the synthesis method of Cr3+-doped ZnAl2O4 for phosphor applications is needed. In this work, two different chelating agents were used in preparing Cr³⁺-doped ZnAl₂O₄ samples. This study may contribute additional knowledge on the effect of chelating agents on the properties of Cr³⁺-doped ZnAl₂O₄ samples. Moreover, the optical properties of these samples were investigated. The suitability of this material for WLED applications was also analyzed.

Materials and Methods

The stoichiometric amounts of zinc nitrate hexahydrate (Zn(NO₃)₂·6H₂O) and aluminum nitrate hexahydrate (Al(NO₃)₃·6H₂O) with a 1:2 Zn-to-Al molar ratio were prepared by dissolving the chemicals in deionized water. Next, 1 mol% of chromium nitrate hexahydrate (Cr(NO₃)₃·6H₂O) was added to the solution while stirring until a homogeneous metal solution was Subsequently, citric/oxalic acid was added to another beaker filled with an ethanol solution under constant stirring. Then, the metal solution was added to ethanol. After that, the chelating agent (i.e., citric acid or oxalic acid solution) was added with vigorous stirring. The solution was heated on a hot plate at 80 °C with constant stirring until the formation of gel. Following that, the gel was put into a crucible and placed into an oven for drying at 150 °C. After the drying process, the gel was calcined for 2 h in a furnace at 800 °C. Finally, the sample was crushed into fine powder for further characterization. The method used was based on the procedure reported by Hussen et al. [16] with some modifications.

To examine the structural properties, X-ray diffraction (XRD) analysis was carried out using an X'Pert PRO PANalytical diffractometer with Cu-K α radiation ($\lambda = 1.54$ Å) with a diffraction angle (2 θ) from 5° to 90° operating at 45 kV and 40 mA. From the XRD data, crystallinity, lattice constant, crystallite size, and microstrain were calculated. Morphology and elemental analysis were carried out

using a scanning electron microscope (SEM-TESCAN VEGA-3 SBU) equipped with an energy-dispersive X-ray spectroscopy (EDS) unit (Oxford INCA X-Max 51-XMX 0021).

The crystallinity index, CI of Cr³⁺-doped ZnAl₂O₄ powder was calculated from the XRD data according to Eq. (1) [17]:

$$CI = \frac{\text{Area of crystalline peaks}}{\text{Area of all peaks}} \times 100\%$$
 (Eq. 1)

The lattice constant, a was calculated using Eq. (2):

$$a = d_{hkl}\sqrt{h^2 + k^2 + l^2}$$
 (Eq. 2)

The interplanar distance, d_{hkl} was calculated using Eq. (3) [16]:

$$d_{hkl} = \frac{\lambda}{2\sin(\theta_{hkl})}$$
 (Eq. 3)

The crystallite size, D of Cr^{3+} -doped $ZnAl_2O_4$ samples was estimated using the following Scherrer's equation [18]:

$$D = \frac{k\lambda}{\beta\cos\theta} \tag{Eq. 4}$$

Where k is the Scherrer's constant (0.9), λ is the wavelength of the X-rays, β is the full width at half-maximum (FWHM) of the X-ray diffraction peak, and θ is the Bragg's angle. The Williamson-Hall (W-H) method was also used to estimate the crystallite size (*D*) and microstrain (ε) using Eq. (5) and Eq. (6) [19, 20]:

$$\beta = \frac{k\lambda}{R\cos\theta} + 4\varepsilon \tan\theta \tag{Eq. 5}$$

By rearranging the above equation:

$$\beta \cos \theta = \frac{k\lambda}{D} + 4\varepsilon \sin \theta \tag{Eq. 6}$$

The plot of β cos θ against sin θ gives the crystallite size corresponding to the y-intercept, and the slope of the graph provides the value of strain.

Results and Discussion

The XRD pattern for Cr³⁺-doped ZnAl₂O₄ indicated that the diffraction peaks of both samples matched with the cubic ZnAl₂O₄ spinel phase (JCPDS 82-1043). The diffraction peaks are sharp and well-defined, indicating a high degree of structural order at long range. **Figure 1** shows the XRD pattern for SC and SO samples. There are nine peaks corresponding to the (220), (311), (331), (400),

(422), (440), (511), (533), and (620) diffraction lines, which have the same peak pattern as the cubic ZnAl₂O₄ spinel phase. The peak positions for both samples are similar according to the standard. No additional peaks were detected in the SO sample, showing that the samples are in a single phase, and chromium ions are successfully incorporated into the ZnAl₂O₄ crystal lattice. The crystallinity indices for the SC and SO samples are approximately 83.40 and 86.88, respectively. This indicates that the sample produced using oxalic acid has better crystallinity.

The FWHM in radians was calculated and is presented in Table 1. The crystallite size values were determined from the five highest peaks, specifically the (220), (311), (440), (422), and (511) peaks, using the Debye-Scherrer equation. The calculated crystallite sizes are 13.66 nm and 12.05 nm for SC and SO samples, respectively. This indicates that the crystallite size of the SC sample is slightly larger compared to the SO sample. This finding is in good agreement with previous work, where the average crystallite size for Cr3+-doped ZnAl2O4 is in the range of 11-12 nm [16]. As shown in Table 1, the lattice constant for all synthesised samples is approximately 8.04 Å, which is slightly lower than the value reported in the literature for zinc aluminate (a = 8.0848 Å, JCPDS 05-0669), as reported bySrinatha et al. [21]. The decrease in lattice constant was also reported after the incorporation of other dopants into the ZnAl₂O₄ host [22, 23].

From the graph in **Figure 2**, the crystallite size can be calculated using the y-intercept value of the W-H

equation, while the slope of the plot corresponds to the microstrain. The microstrains for SC and SO samples are 0.0025 and 0.0017, respectively. Based on the findings, SO has a smaller crystallite size of 15.94 nm, compared to SC, which has a crystallite size of 23.11 nm. This result shows that using oxalic acid as a precursor can reduce the crystallite size. Based on Table 1, it is shown that the crystallite size calculated using the W-H equation is larger than calculated using the Debye-Scherrer equation. This is because the W-H equation considers the positive strain developed in samples [16].

The SEM images of Cr3+-doped ZnAl2O4 samples at a magnification of 5,000× are shown in Figure 3. The figure reveals that sample SC is agglomerated, and the particles are attached to each other with clear grain boundaries. For sample SO, the particles are less agglomerated, with an irregular particle size distribution. This finding indicates that different chelating agents affect the morphology and particle size of the samples. A similar finding was reported by Monfared et al. [24], who noted that different types of carboxylic acids directly affect the size and catalytic activity of magnetite nanoparticles. The carboxylate groups of citric acid and oxalic acid have a strong coordination affinity to metal ions, which preferentially attach the carboxylate groups to the surface of the crystals and prevent them from aggregating into large single crystals. Given their strong complexation with metal ions, the carboxylate groups can anchor on the particle surface during the solvothermal reaction, thereby enhancing the dispersibility of ZnAl₂O₄ particles.

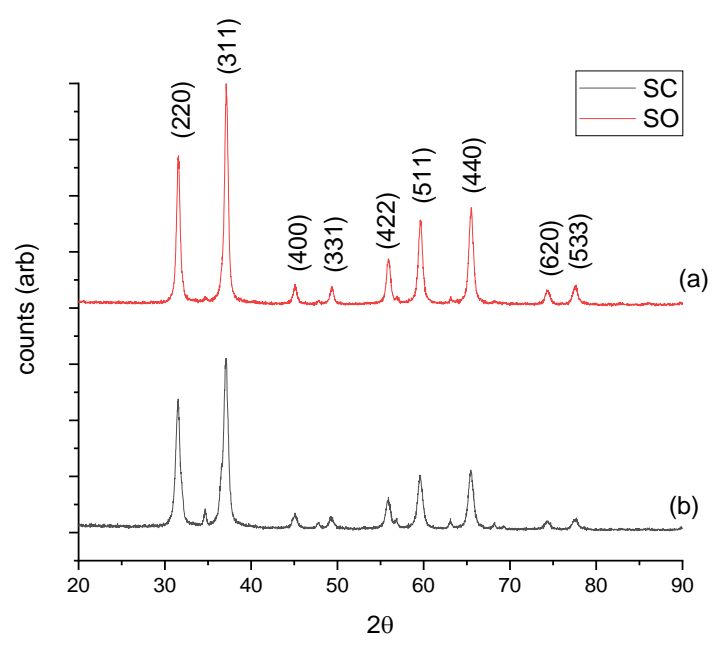


Figure 1. XRD pattern, a) SC and b) SO of Cr^{3+} doped $ZnAl_2O_4$ sample Table 1. Structural parameters of Cr^{3+} -doped $ZnAl_2O_4$ samples calculated from XRD data.

Sample	Crystallinity, <i>CI</i>	Lattice Constant, a (Å)	Crystallite size, D using Scherrer (nm)	Crystallite Size, <i>D</i> using W-H plot (nm)	Micro Strain, ε (×10 ⁻³)
SC	83.40	8.0449	13.66	23.11	2.5
SO	86.88	8.0391	12.05	15.94	1.7

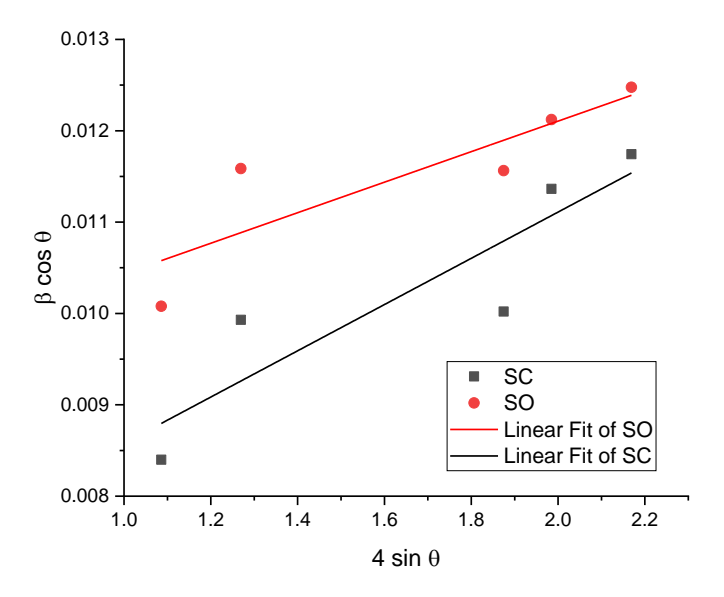
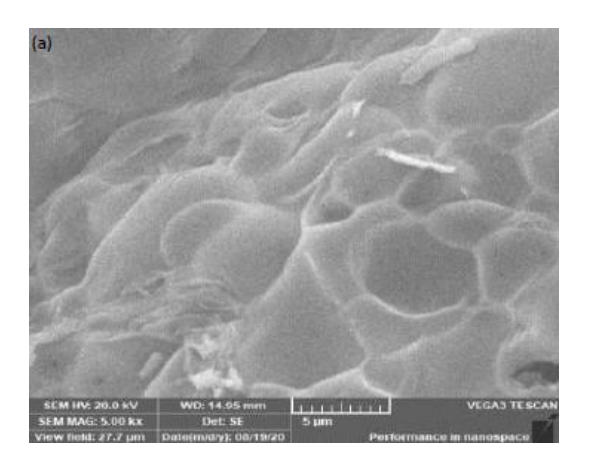


Figure 2. W-H plot of Cr³⁺-doped ZnAl₂O₄ samples



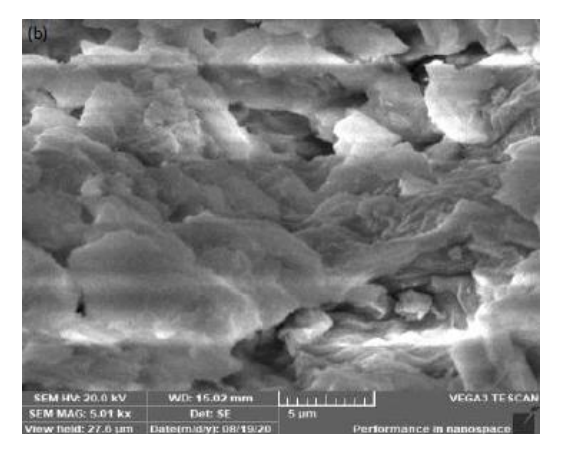


Figure 3. SEM micrographs of Cr³⁺-doped ZnAl₂O₄ samples: a) SC and b) SO.

As shown in Figure 4(a) and Figure 4(b), oxalic acid and citric acid contain two and three carboxylic acid groups, respectively. The additional carboxylic group in citric acid facilitates the formation of larger crystals compared to oxalic acid, indicating that a greater number of carboxylate groups promotes more extensive aggregation, with each oxygen atom coordinating to metal atoms. In contrast, oxalic acid, which has only two carboxylic groups, provides fewer sites for hydrogen bonding, thereby limiting its ability to stabilise a larger, more complex crystal structure. Furthermore, due to the higher acidity of

oxalic acid compared to citric acid, it creates a more favourable environment for the formation of smaller crystallites of $ZnAl_2O_4$.

The EDS analysis was carried out to validate the constituent elements in the samples. **Figure 5** shows the EDS spectrum of Cr³⁺-doped ZnAl₂O₄ for both samples. The analysis confirmed the presence of the predicted elements of Zn, Al, O, and Cr. The weight and atomic proportions of Cr³⁺-doped ZnAl₂O₄ sample components are shown in **Table 2**. The amount of Cr dopant for sample SO is nearly

equivalent to the amount prepared, while sample SC exhibits a lower amount. Furthermore, the Zn-to-Al weight percentage ratio differs from the calculated stoichiometric ratio. The accuracy of EDS measurement can be improved by analysing more sites on the sample surface and using more accurate method.

In order to assess the suitability of the sample, it is important to analyse its optical properties. In this study, the energy band gap of the samples was determined by constructing a Tauc plot, as shown in **Figure 6.** The energy band gaps for SC and SO are 2.89 and 3.0 eV, respectively. The result is in good agreement with a previous study, where the range of energy band gap for similar materials is between 2.72 and 3.02 eV [25]. Additionally, the band gap value is influenced by the calcination temperature during sample synthesis. This value is also comparable to that of zinc oxide, which is widely used as a photocatalyst for the degradation of organic dyes in water [26]. Therefore, this result highlights the suitability of these samples for similar applications.

Figure 4. The structure of a) oxalic acid and b) citric acid

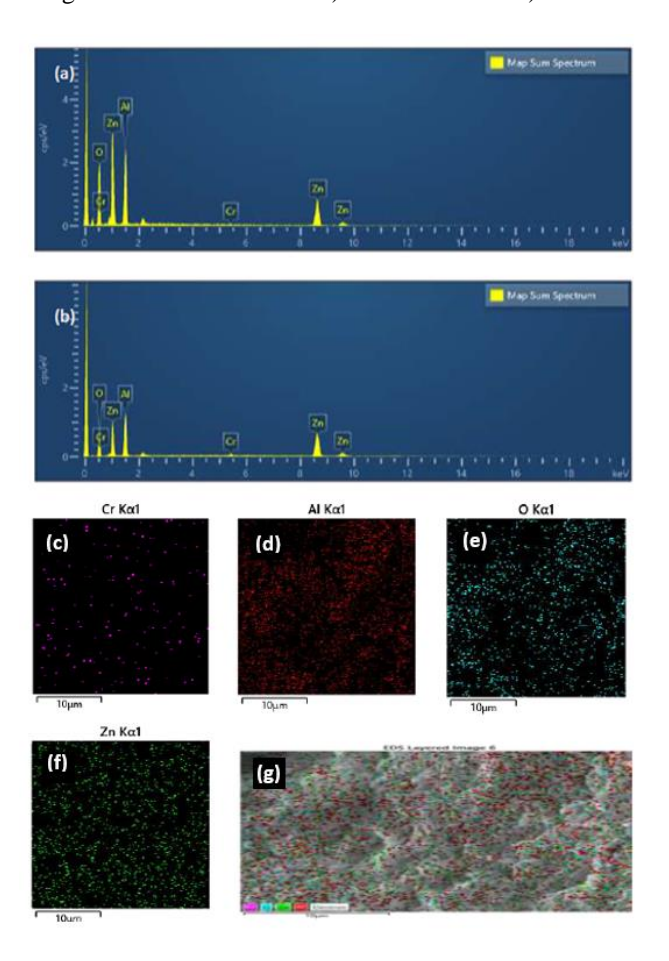


Figure 5. EDS spectrum of Cr³⁺ doped ZnAl₂O₄ samples. a) SC and b) SO. Representative EDS elemental mapping c) Cr, d) Al, e) O, f) Zn and g) layered image

Table 2. The weight and atomic percentage of elements for Cr³⁺-doped ZnAl2O4 sample.

Samples	Elements	Weight (wt.%)	Atomic (at.%)
\mathbf{SC}	Zn	34.34	13.66
	Al	29.86	28.78
	O	35.23	57.27
	Cr	0.57	0.29
so	Zn	53.44	25.12
	Al	17.00	19.36
	O	28.63	54.98
	Cr	0.93	0.55

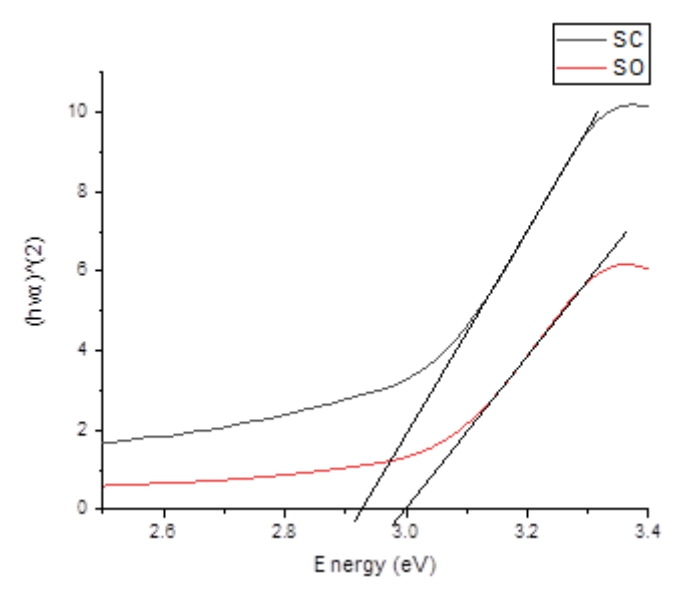


Figure 6. Tauc plot to determine the optical band gap for Cr³⁺-doped ZnAl₂O₄ samples

The photoluminescence spectra of the samples are depicted in Figure 7. Based on the results, both samples exhibit broad emission peaks in the blue and red regions. According to the CIE diagram (see inset in Figure 7), the CIE 1931 coordinates are (0.2522, 0.21113) and (0.29003, 0.27166) for the SC and SO samples, respectively. Notably, the CIE coordinates for the SO sample are near the white region, which can potentially be applied as a phosphor for generating white light. Figure 8 shows the lifetime plot for the SC and SO samples, which are approximately 0.51 ms and 0.65 ms, respectively. These lifetime values are significantly longer than the cell autofluorescence, which is approximately 20 ns, as well as the signal of cell fluorescence or other background, which can be easily subtracted using a time-gated imaging system. Therefore, this sample demonstrates potential as a biomarker bioimaging, as reported in a previous study [27].

Conclusion

In this study, Cr3+-doped ZnAl2O4 samples were successfully synthesised via the sol-gel method using citric acid and oxalic acid as chelating agents. Based on the XRD analysis, the samples exhibit a cubic ZnAl₂O₄ spinel phase. The SO sample has a smaller crystallite size and better crystallinity compared to the SC sample. The SEM analysis indicated that the SO sample exhibited better size distribution than the SC sample, highlighting the suitability of oxalic acid as a chelating agent. Moreover, the EDS analysis confirmed the presence of Zn, Al, O, and Cr. Additionally, the CIE coordinates near the white region suggest the potential of this material as a phosphor for WLED applications. In addition to its use as a phosphor, this material can also be used as a photocatalyst and biomarker. Future studies could explore different techniques or other doping elements to further enhance the optical properties of Cr³⁺doped ZnAl₂O₄.

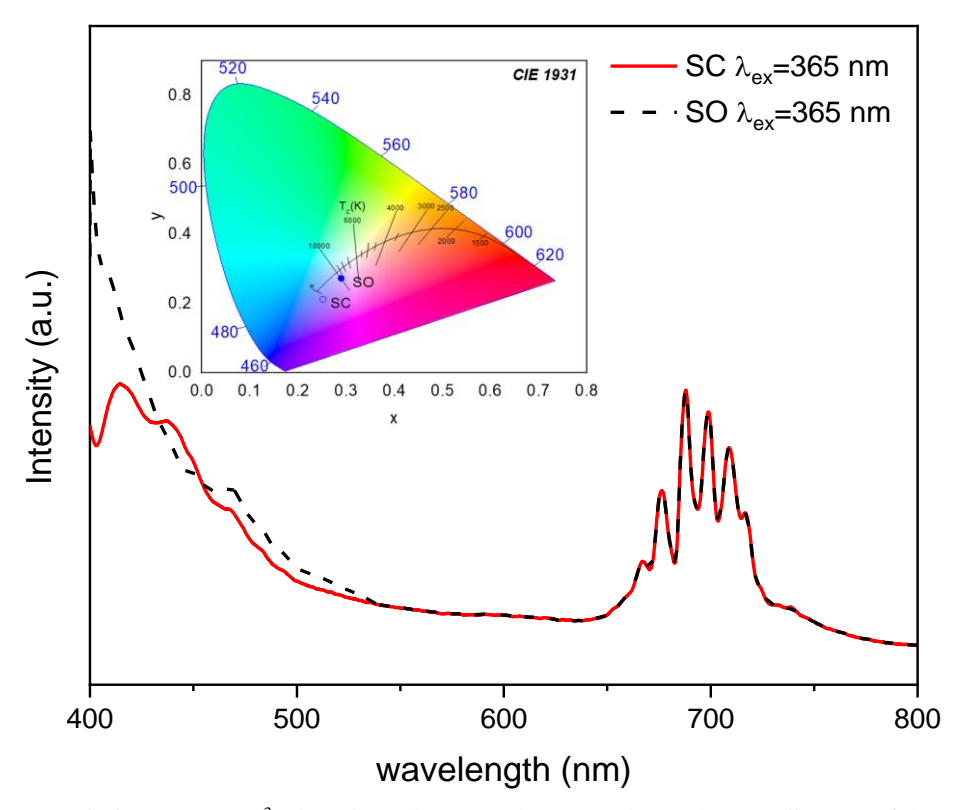


Figure 7. Emission spectra Cr³⁺-doped ZnAl₂O₄ samples. Inset shows the CIE diagram of the sample

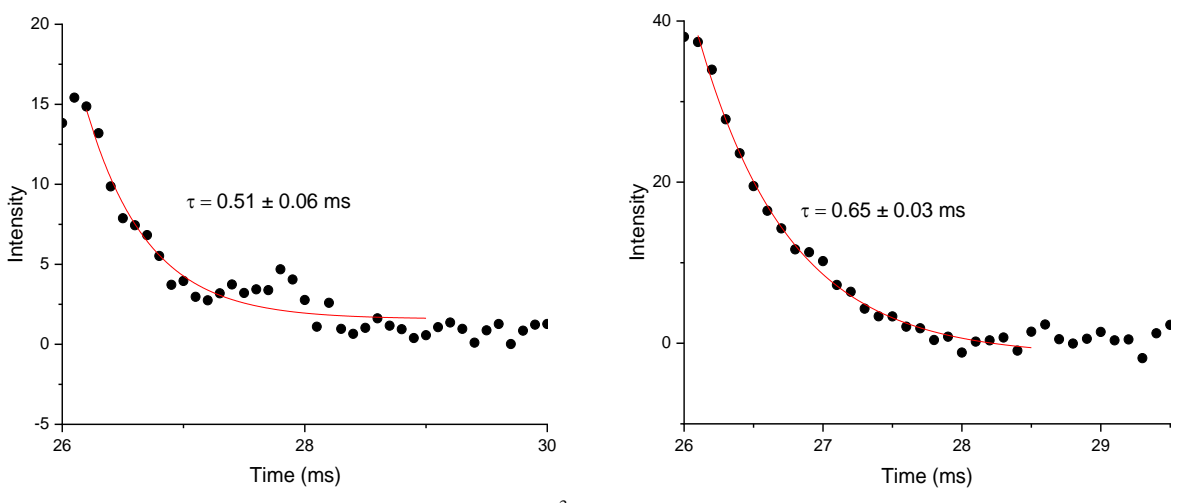


Figure 8. Photoluminescence lifetime of Cr³⁺-doped ZnAl₂O₄ samples SC (left) and SO (right)

Acknowledgements

The author would like to acknowledge Universiti Teknologi MARA Pahang, Universiti Teknologi MARA Shah Alam, Universiti Teknologi MARA Dengkil for research facilities.

References

Strachowski, T. Grzanka, E. Mizeracki, J. Chlanda, A. Baran M., Małek, M. and Niedziałek, M. (2022). Microwave-assisted hydrothermal synthesis of zinc-aluminum spinel

ZnAl₂O₄. Materials, 15: 245.

- Srinatha, N. Kumar, K. R. Kumar, M. S. Madhu, A. and Angadi, B. (2022). A novel combustion fuel for the synthesis of nanocrystalline ZnAl₂O₄ particles based on the thermodynamic correlations and their structural and optical studies. *Ceramics International*. 48: 3669-3675.
- 3. Singh, V. Chakradhar, R. Rao, J. and Kim, D. K. (2008). Characterization, EPR and luminescence studies of ZnAl₂O₄: Mn

- phosphors. *Journal of Luminescence*, 128: 394-402
- Balakrishnan, S. Tiwari, A. Iyer, S. Kumbhar, P. Pusdekar, A. and Ugemuge, N. (2024). Energy transfer from Ce³⁺ to Eu³⁺ in the spinel structure of ZnAl₂O₄ phosphor for optoelectronic applications. *Radiation Effects and Defects in Solids*, 179: 799-810.
- Yuvaraj, S. Revathi, S. Kumar, A. Anitha, G. Al-Enizi, A. M. and Pandit, B. (2023). Impact of Cd²⁺ substituted ZnAl₂O₄ spinel nanoparticles on structural, optical, morphological, magnetic and nonlinear optical behaviour. *Optical Materials*, 145: 114423.
- Tran, M. Trung, D. Tu, N. Anh, D. Thu, L. Du, N. (2021). Single-phase far-red-emitting ZnAl₂O₄: Cr³⁺ phosphor for application in plant growth LEDs. *Journal of Alloys and Compounds*, 884:16107.
- Huang, S. Wei, Z. Wu, X. and Shi, J. (2020). Optical properties and theoretical study of Mn doped ZnAl₂O₄ nanoparticles with spinel structure. *Journal of Alloys and Compounds*, 825:154004
- 8. Habibi, M. K. S. M. Alhaji A. and Zare, M. (2021). ZnAl₂O₄: Ce³⁺ phosphors: Study of crystal structure, microstructure. *Journal of Molecular Structure*, 1228: 129769.
- Srinatha, N. Reddy, S. S. Gurushantha, K. Al-Dossari, M. Manjunatha, S. O. and Madhu, A. (2024). Exploring the impact of Sm³⁺ doping on the structural, optical, and photocatalytic properties of ZnAl₂O₄ spinels. *Ceramics International*, 50: 37742-37753.
- Venkatesh, R. Yadav, L. R. Dhananjaya N. and Jayasheelan A. (2022). Green combustion synthesis of ZnAl₂O₄: Eu³⁺ nanoparticle for photocatalytic activity. *Materials Today: Proceedings*, 49:583-587.
- 11. Chen, Z. Zhao, X. and Wei, S. (2021). Comparative study on sol-gel combined with a hydrothermal synthesis of ZnAl₂O₄ and ZnO/ZnAl₂O₄ nanocomposites and its photoluminescence properties and antibacterial activity. *Optik*, 242:167151.
- 12. Gurugubelli, T. R. Babu, B. and Yoo, K. (2021). Structural, optical, and magnetic properties of cobalt-doped ZnAl₂O₄ nanosheets prepared by hydrothermal synthesis. *Energies*, 14:2869.
- Lakshminarayana, G. and Wondraczek, L. (2011). Photoluminescence and energy transfer in Tb³⁺/Mn²⁺ co-doped ZnAl₂O₄ glass ceramics. *Journal of Solid State Chemistry*, 184: 1931-1938.
- 14. Sharma, S. Gourier, D. Viana, B. Maldiney, T. Teston, E. and Scherman, D.(2014). Persistent luminescence of AB₂O₄: Cr³⁺ (A= Zn, Mg, B= Ga, Al) spinels: new biomarkers for in vivo

- imaging. Optical Materials, 36: 1901-1906.
- 15. Zhou, Y. Li, X. Seto T. and Wang, Y. (2021). A high efficiency trivalent chromium-doped near-infrared-emitting phosphor and its NIR spectroscopy application. *ACS Sustainable Chemistry & Engineering*, 9: 3145-3156.
- Hussen, M. K. Dejene, F. B. and Tsega, M. (2019). Effect of pH on material properties of ZnAl₂O₄: Cr³⁺ nano particles prepared by solgel method. *Journal of Materials Science: Materials in Electronics*, 30: 10191-10201.
- 17. Pan, Y. Tang, Y. Yin, X. Qiang, M. Yao, X. and Zhang, D. (2024). ZnAl₂O₄: Mn²⁺ transparent phosphor ceramic with narrow-band green emission by spark plasma sintering. *Journal of Luminescence*, 265: 120198.
- Shang-Pan, H Zhi-Qiang, W. Xiao-Juan W. and Ji-Wen, S. (2020). Optical properties of Cr doped ZnAl₂O₄ nanoparticles with Spinel structure synthesized by hydrothermal method. *Materials Research Express*, 7: 015025.
- Javed M. and Akbar, N. (2023). The structural investigation and photocatalytic application of sol-gel auto-combustion derived ZnAl₂O₄ spinel for the degradation of organic dye. *Kashmir Journal of Science*, 2: 24-37.
- Nirmala, T. S. Iyandurai, N. Yuvaraj, S. and Sundararajan, M. (2020). Effect of Cu²⁺ ions on structural, morphological, optical and magnetic behaviors of ZnAl₂O₄ spinel. *Materials Research Express*, 7: 046104.
- Srinatha, N. Rudresh Kumar K. J., Suresh Kumar, M. R. Madhu A. and Angadi, B. (2022). A novel combustion fuel for the synthesis of nanocrystalline ZnAl₂O₄ particles based on the thermodynamic correlations and their structural and optical studies. *Ceramics International*, 48: 3669-3675.
- Akika, F. Z. Benamira, M. Lahmar, H. Trari, M. Avramova, I. and Suzer, Ş. (2020). Structural and optical properties of Cu-doped ZnAl₂O₄ and its application as photocatalyst for Cr(VI) reduction under sunlight. Surfaces and Interfaces, 18: 100406.
- 23. Menon, S. G. Kunti, A. K. Kulkarni, S. D. Kumar, R. Jain, M. Poelman, D. (2020). A new microwave approach for the synthesis of green emitting Mn²⁺-doped ZnAl₂O₄: A detailed study on its structural and optical properties. *Journal of Luminescence*, 266: 117482.
- 24. Hosseini-Monfared, H. Parchegani, F. and Alavi, S. (2015). Carboxylic acid effects on the size and catalytic activity of magnetite nanoparticles. *Journal of Colloid and Interface Science*, 437: 1-9.
- 25. Mohanty, P. Mohapatro, S. Mahapatra, R. and Mishra, D. K. (2021). Low cost synthesis route of spinel ZnAl₂O₄. *Materials Today*:

- Proceedings, 35: 130-132.
- 26. Bi, T. Du, Z. Chen, S. He, H. Shen, X. and Fu, Y. (2023). Preparation of flower-like ZnO photocatalyst with oxygen vacancy to enhance the photocatalytic degradation of methyl orange. *Applied Surface Science*, 614: 156240.
- Razali, W. A. W. Sreenivasan, V. K. Bradac, C. Connor, M. Goldys, E. M. and Zvyagin, A. V. (2016). Wide-field time-gated photo luminescence microscopy for fast ultrahighsensitivity imaging of photoluminescent probes. *Journal of Biophotonics*, 9: 848-858.